2009 ASEE Northeast Section Conference
April 3-4, 2009, Bridgeport, CT

Validation of Turbulence Models in STAR-CCM+ by N.A.C.A. 23012 Airfoil Characteristics

K. Ren*, J. Hu*, X. Xiong, L. Zhang**, and J. Wei†**
***Department of Mechanical Engineering, University of Bridgeport**
****Department of Electrical Engineering, University of Bridgeport**
† Kaman Aerospace

Abstract

Computational fluid dynamics (CFD) provides the helicopter designer with an analysis tool capable of evaluating complex rotary wing aerodynamics. There is a wide range of turbulence models developed to simulate the viscous turbulent aerodynamics flow, however, more accurately and efficiently modeling turbulence is still a challenge in today's CFD research and applications. Turbulent transport processes are strongly problem-dependent, which can only give an approximate description with a particular set of empirical constants for a certain range of flows. It is also reported that the same turbulence model predict very different results in different commercial CFD codes. Therefore, the development and application of turbulent models rely on experimental data for validation. In this project, three turbulence models, which are *K*-ε, *K*-ω and Reynolds Stress Transport turbulence models are tested and validated in the state-of-art CFD code STAR-CCM+ by simulating the turbulent flow over an N.A.C.A. 23012 airfoil with an N.A.C.A. 23012 external-airfoil flap. The predicted results are compared with wind tunnel data for flow over the airfoil with an external-airfoil flap at different attack angle and flap deflections.

Introduction

The development and application of CFD has become a key to the success of the NASA, air force, and aerospace industry. It has been a constant effort of NASA to develop, validate, and support CFD tools to increase their capability in the analysis, design, and development of aerospace vehicles and components [1]. Computational fluid dynamics (CFD) provides the helicopter designer with an analysis tool capable of evaluating complex rotary wing aerodynamics [2]. There is a wide range of turbulence models developed to simulate the viscous turbulent aerodynamics flow, however, more accurately and efficiently modeling turbulence is still a challenge in today's CFD research and applications [3,4]. Turbulent transport processes are strongly problem-dependent, which can only give an approximate description with a particular set of empirical constants for a certain range of flows. It is also reported that the same turbulence model predict very different results in different commercial CFD codes [5]. Therefore, the development and application of turbulent models rely on experimental data for validation [6]. In this project, three turbulence models, which are *K*-ε, *K*-ω and Reynolds Stress Transport turbulence models, are tested and validated in the state-of-art CFD code STAR-CCM+ by simulating the turbulent flow over an N.A.C.A. 23012 airfoil with an N.A.C.A. 23012 external-airfoil flap [7]. The predicted results are compared with wind tunnel data for flow over the airfoil with an external-airfoil flap at different attack angle and flap deflections.

Figure 1 shows the NACA 23012 airfoil with an NACA 23012 external-airfoil flap with flap deflected δ_f and at an attack angle α.

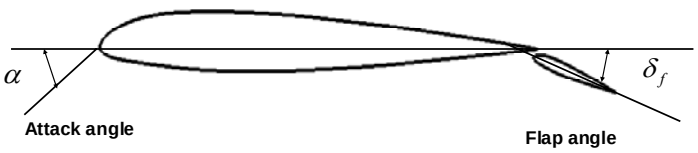

Fig. 1 A NACA 23012 airfoil with an NACA 23012 external-airfoil flap with flap deflected at δ_f at an attack angle α.

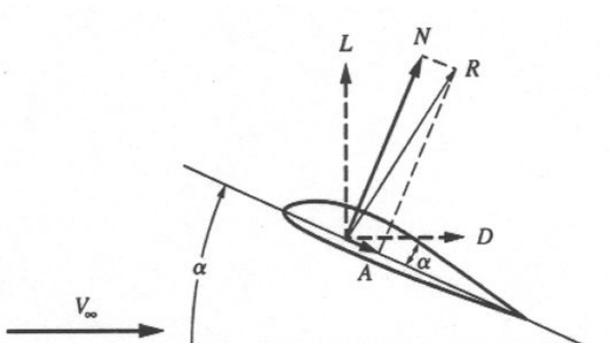

Fig. 2 A schematic diagram of an airfoil and the resultant aerodynamic force when a flow attack it with an angle α and velocity V_∞ [8].

Figure 3 shows an airfoil in a flow at a free stream velocity of V_∞ and an attack angle α [8]. The resultant aerodynamic force R can be split into two components life force L and drag force D. The resultant force R can also be split into normal force N and axial force A. The normal force N and the axial force A can be calculated by

$$N = L\cos\alpha + D\sin\alpha$$
$$A = -L\sin\alpha + D\cos\alpha \quad (1)$$

As the wind tunnel data in Reference [7] presented normal force coefficient, but not the lift coefficient. the normal coefficient C_N is calculated from lift coefficient C_L and drag coefficient C_D by

$$C_N = C_L\cos\alpha + C_D\sin\alpha \quad (2)$$

The lift coefficient C_L, and drag coefficient C_D, normal force coefficient C_N, and pressure coefficient C_P are defined as

$$C_L = \frac{L}{\frac{1}{2}\rho_\infty V_\infty^2 (c_w + c_f)}, \quad C_D = \frac{D}{\frac{1}{2}\rho_\infty V_\infty^2 (c_w + c_f)}, \quad C_N = \frac{N}{\frac{1}{2}\rho_\infty V_\infty^2 (c_w + c_f)}, \quad c_p = \frac{p - p_\infty}{\frac{1}{2}\rho_\infty V_\infty^2} \quad (3)$$

where c_w chord length of the main airfoil and c_f is the chord length of the external flap; ρ_∞ is the free stream density; p is the pressure; and p_∞ is the free stream pressure.

Turbulence Models in STAR-CCM+

K-Epsilon Turbulence model

A K-ε turbulence model is a two-equation model in which transport equations are solved for the turbulent kinetic energy κ and its dissipation rate ε [9]. K-Epsilon turbulence model has been widely used in industrial for several decades. The Realizable Two-Layer K-Epsilon model

is selected for this project. This model combines the Realizable K-Epsilon model with the two-layer approach. The Realizable K-Epsilon mode is substantially better than the standard K-Epsilon model for many applications [9]. The two-layer approach enables it to be used with fine meshes that resolve the viscous sublayer.

K-Omega Turbulence model

A *K*-ω model is a two-equation model and it is an alternative to the *K*-ε. One advantage of *K*-ω model is its improved performance for boundary layers under adverse pressure gradients. The boundary layer computation is very sensitive to the values of turbulent kinetic energy quantity in the free stream in the original form of *K*-ω model. In this project, we used SST (shear-stress transport) K-omega model which effectively blends a *K*-ε model in the far-field with a *K*-ω model near the wall. It also introduced a modification to the linear constitutive equation. The SST model has been widely application in the aerospace industry, where viscous flows are typically well resolved and turbulence models are generally applied throughout the boundary layer [9]. All-y^+ wall treatment is selected.

Spalart-Allmaras Turbulence model

A Spalart-Allmaras Turbulence models solve a single transport equation that determines the turbulence viscosity. They are implemented in an unstructured solver and widely used in the aerospace industry. Spalart-Allmaras Turbulence models are well suited to simulate attached boundary layers and flow with mild separation, but are not suited to predict spreading rates for plane, round jets, flow involving complex recirculation and body forces [9]. We can use Spalart-Allmaras model for a plain airfoil, but it is hard to achieve convergence for flow over an airfoil with a flap. Therefore, Spalart-Allmaras model is not used in the current study.

Reynolds Stress Transport (RST) Turbulence model

Reynolds Stress Turbulence models, also known as second-moment closure models, are the most complex turbulence models in STAR-CCM+ [9]. They solve transport equations for all components of the specific Reynolds stress tensor. They can account for anisotropy effects due to strong swirling motion, streamline curvature, rapid changes in strain rate and secondary flows in ducts. The Quadratic Pressure Strain RST model is chosen in this study.

Problem Specification

The chord length of the NACA 23012 airfoil is 20.0 inches and the chord length of the NACA 23012 flap is 4.0 inches. The main stream air velocity is taken as 35.71 m/s and the air properties are taken at standard sea-level conditions according to the wind tunnel set up. The Reynolds number, based on the combination of the main airfoil an flap chords, is 1.46×10^6. The attack angles are chosen according to the experimental data available for comparison. Three turbulence models, *K*-ε, *K*-ω and RST, are used to calculate the aerodynamic characteristics of the flapped airfoil. Three flap deflections are studied, as shown in Fig. 4, at $\delta_f = 0^o$, $\delta_f = 20^o$ and $\delta_f = 40^o$.

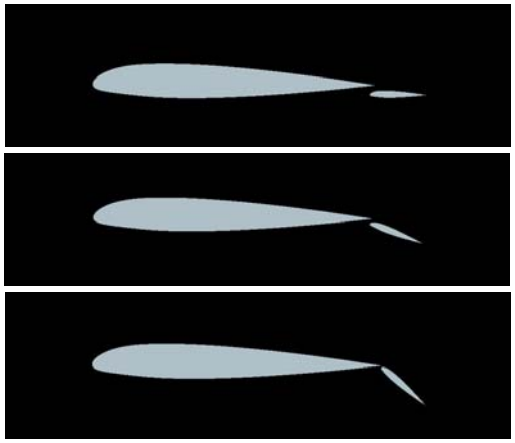

Fig. 3 Airfoil and external flap with flap defected at (a) $\delta_f = 0^o$, (b) $\delta_f = 20^o$, (c) $\delta_f = 40^o$.

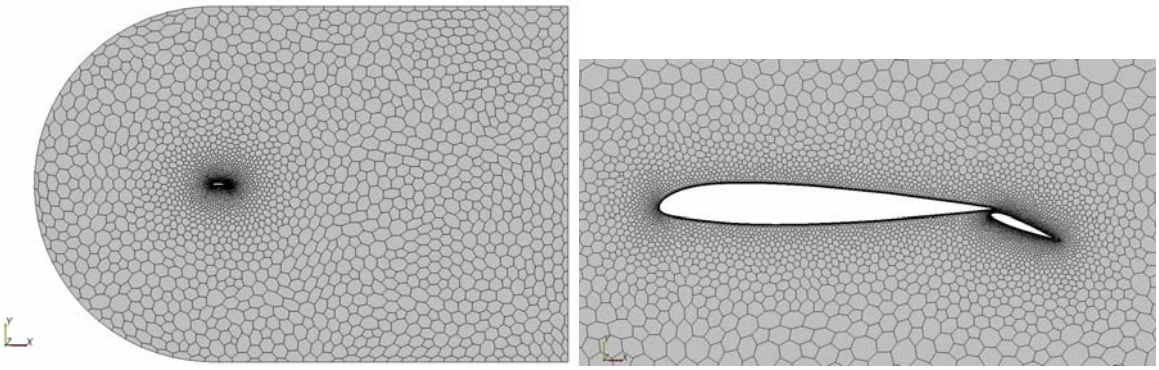

(a) (b)

Fig. 4 Computational mesh: (a) full view and (b) close view of the airfoil and flap.

The unstructured polyhedral mesh is generated in STAR-CCM+. As shown in Fig. 3, finer mesh is used around the airfoil and flap, especially in the leading edge and trailing edge regions. The y^+ of the first near wall cell is in the range of 0.5 to 30 at the airfoil and flap surface. All-y^+ wall treatment has been selected for both *K*-*ε*, *K*-*ω* models, which offers the most mesh flexibility with good results on fine meshes ($y^+ < 1$) and intermediate meshes ($1 < y^+ < 30$). As high-y^+ wall treatment for the Quadratic Pressure Strain RST model, the current first cell height is too low for the RST model.

In the following results and discussion section, at each flap deflection, a typical flow field is presented and the normal force coefficient and pressure coefficient curves obtained from the three turbulent models are compared with the wind tunnel data [7]. Lift coefficient is more commonly known, but it is not shown here. As the attack angle is low in the current study, the lift coefficient C_L is very close to the normal force coefficient C_N.

Results and Discussion

1. Flap deflected 0^o

Figure 5 shows the normal force coefficient C_N at various attack angles with flap deflected 0^o. For the airfoil with a 0^o deflected flap, the normal force coefficient obtained from all the

three turbulence models agree well with the experimental results at attack angles ranging widely from -8.0° to 10.0°. RST model gives the best results while *K*-ε and *K*-ω models give similar results. In Fig. 6, the pressure coefficients predicted by the three models are very close to each other and the experimental data at 2.32° attack angle. The velocity magnitude contour obtained by *K*-ω model shows the flow is still attached to both the airfoil and flap at 2.32° attack angle in Fig. 7.

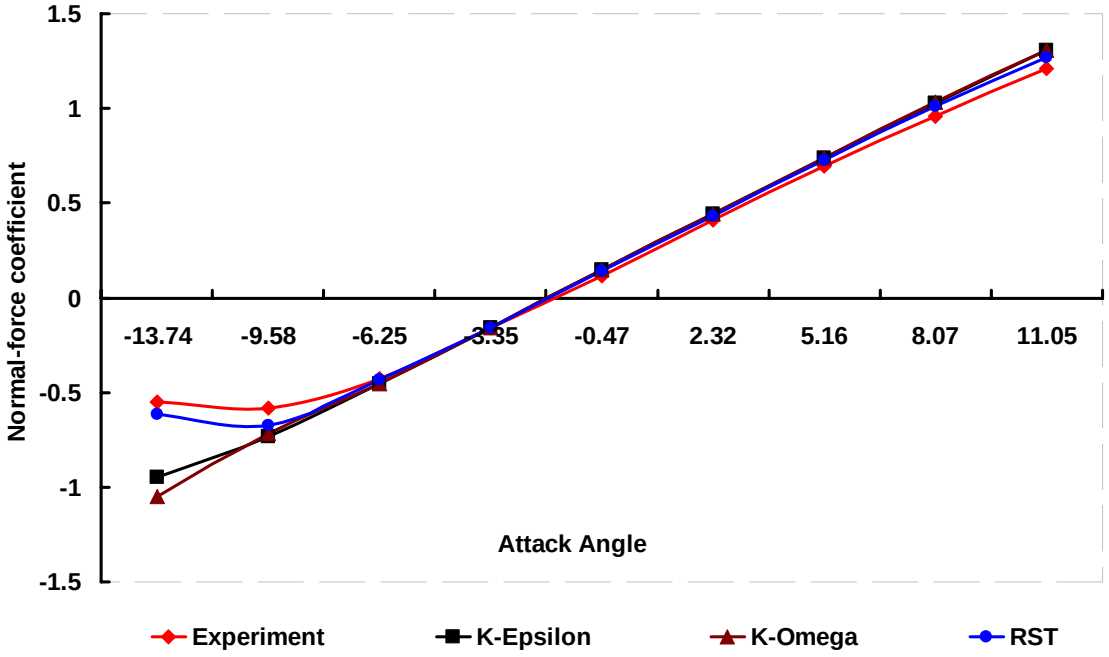

Fig. 5 Normal force coefficient C_N at various attack angles with flap deflection of 0°.

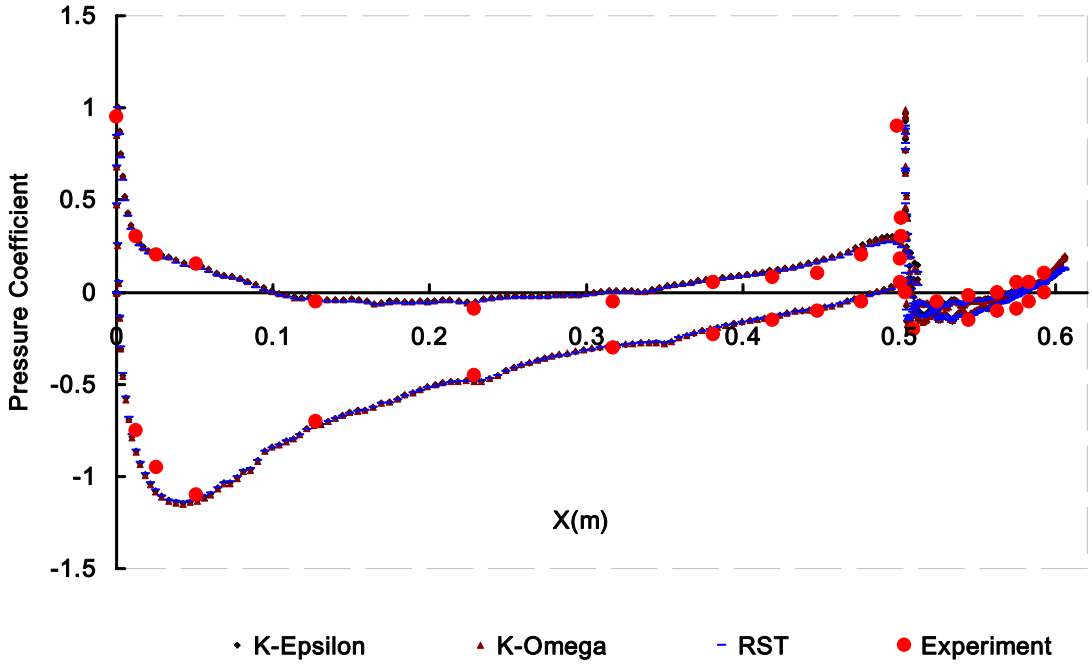

Fig. 6 Pressure coefficient C_p at 2.32° attack angle with 0° flap deflection.

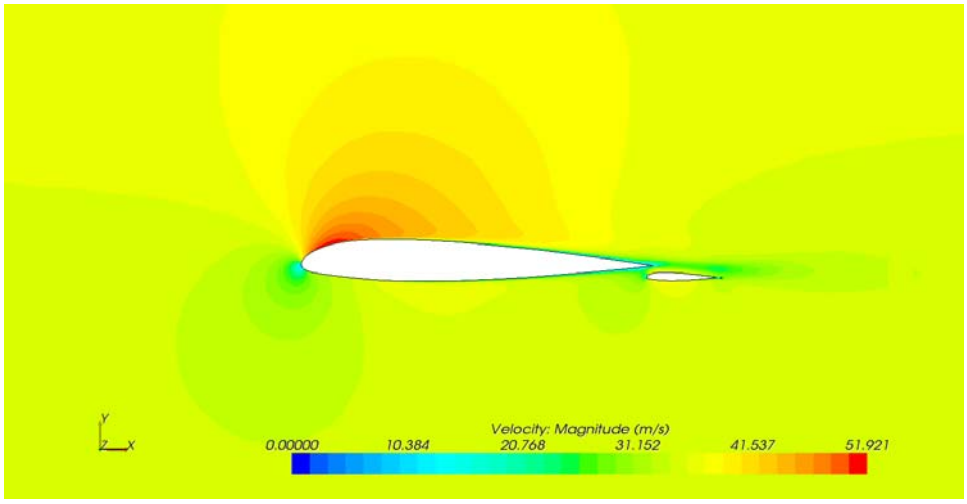

Fig. 7 Velocity magnitude contour at 2.32^o attack angle with 0^o flap deflection.

2. Flap deflected 20^o

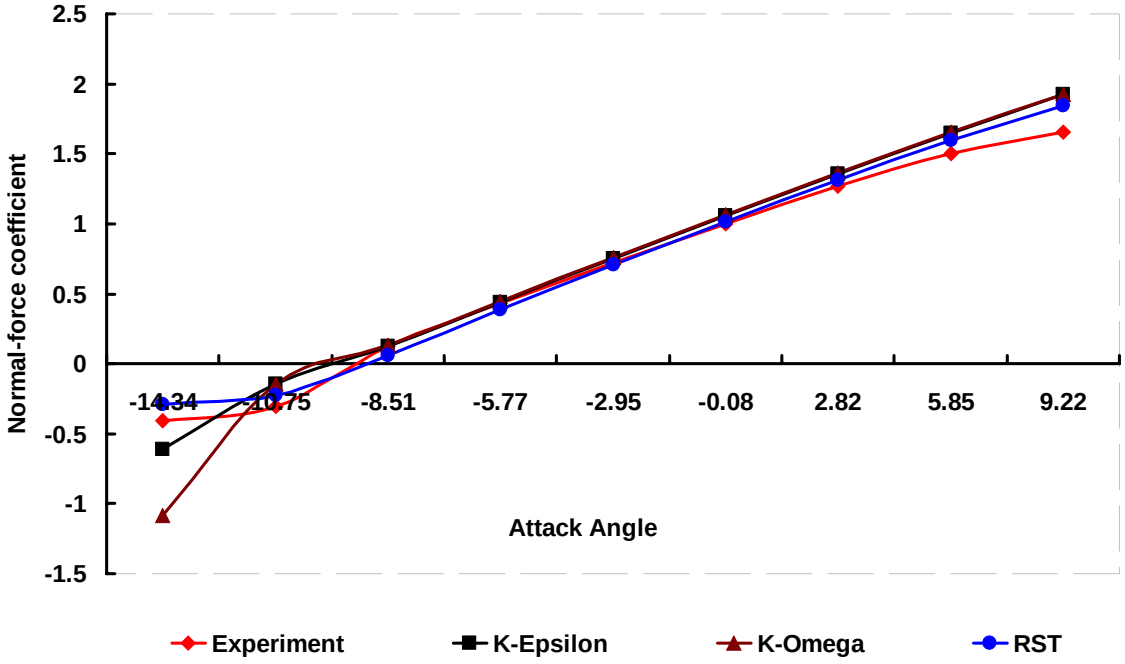

Fig. 8 Normal force coefficient C_N at various attack angles with flap deflection of 20^o.

In Fig. 8, the calculated normal force coefficient C_n agrees well with the experimental value at an attack angle range of -8.0^o and 2.8^o when the flap is deflected 20^o. The pressure coefficients match the experimental data very well at -0.08^o attack angle in Fig. 9, but they slightly depart from the experimental data at 9.22^o attack angle in Fig. 10. The velocity magnitude contour obtained by *K-ω* model shows the flow is still attached to both the airfoil and flap at -0.08^o attack angle in Fig. 11. The discrepancies are prominent in the leading edge of both the airfoil and flap. Transitions of the boundary layer from laminar to turbulent are neglected at the leading edges of the airfoil and flap in this study. According to [10], transition effects play a

big role in accurately simulating flow around airfoils at low Reynolds number. RST model still gives the best results while *K*-ε and *K*-ω models give similar results.

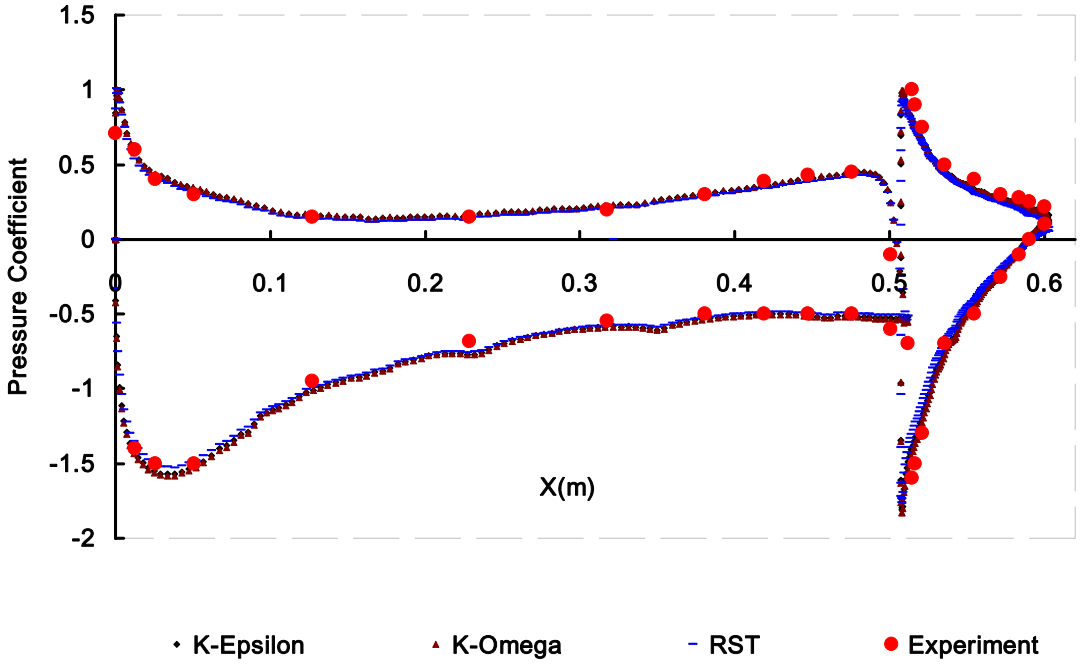

Fig. 9 Pressure coefficient C_p at -0.08^o attack angle with 20^o flap deflection

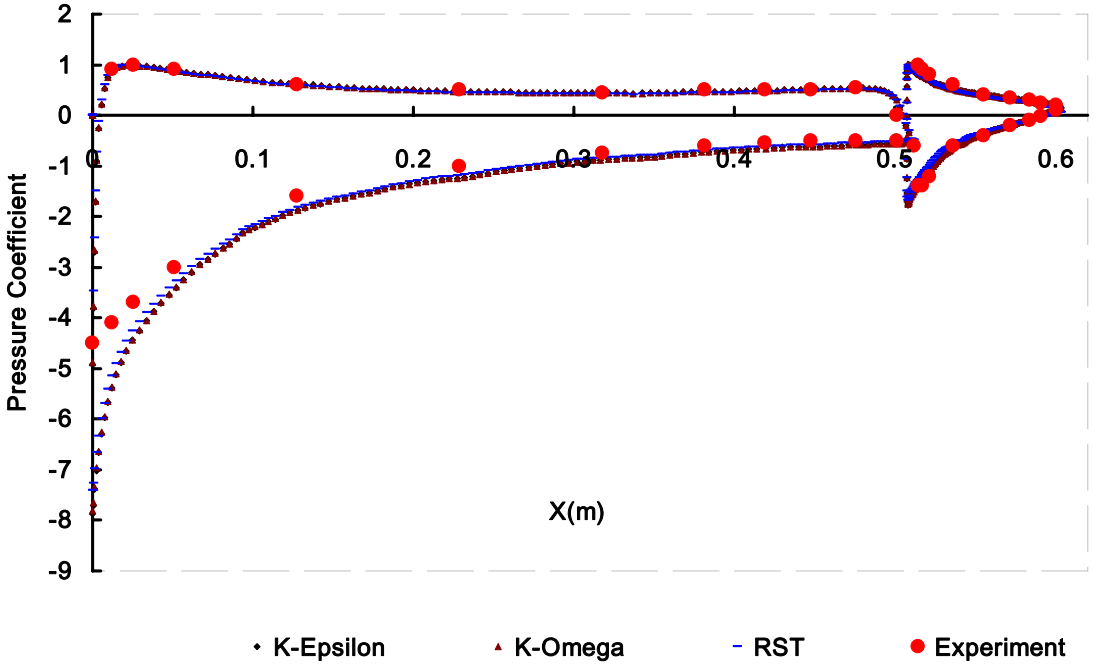

Fig. 10 Pressure coefficient C_p at 9.22^o attack angle with 20^o flap deflection

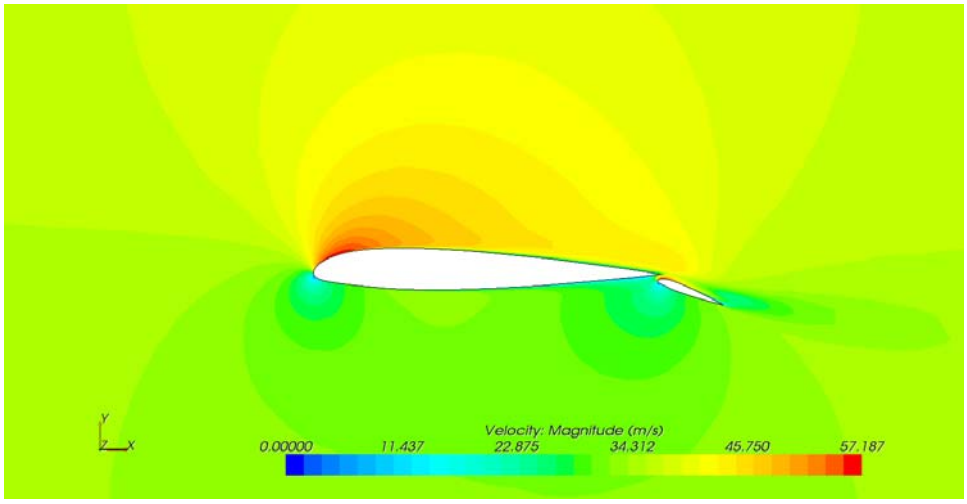

Fig. 11 Velocity magnitude contour at -0.08^o attack angle with 20^o flap deflection

3. Flap deflected 40^o

When the flap deflection increases, the discrepancies between the CFD results and experimental results increase. The CFD results depart from the experimental results at most attack angles for 40^o flap deflection, as shown in Fig. 12. The pressure coefficient curves in Figs. 13 and 14 show significant discrepancies, especially in the leading edges of both the airfoil and flap. The velocity magnitude contour obtained by *K*-ω model shows the flow is separated from the flap 9.59^o attack angle in Fig. 15. The results generated by *K*-ω are slightly better than those by RST model, while the errors of the *K*-ε model are remarkable. As this study used the same set of mesh for various attack angles and flap deflections, part of the errors may come from the lacking of mesh resolution in the wake region.

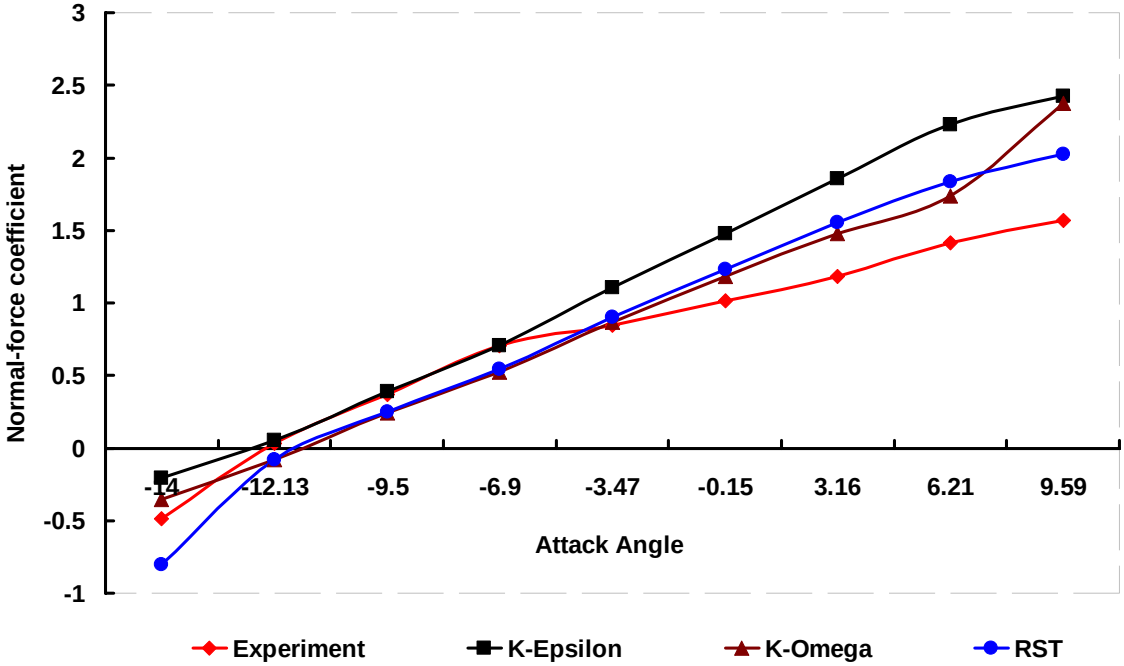

Fig. 12 Normal force coefficient C_N at various attack angles with flap deflection of 40^o.

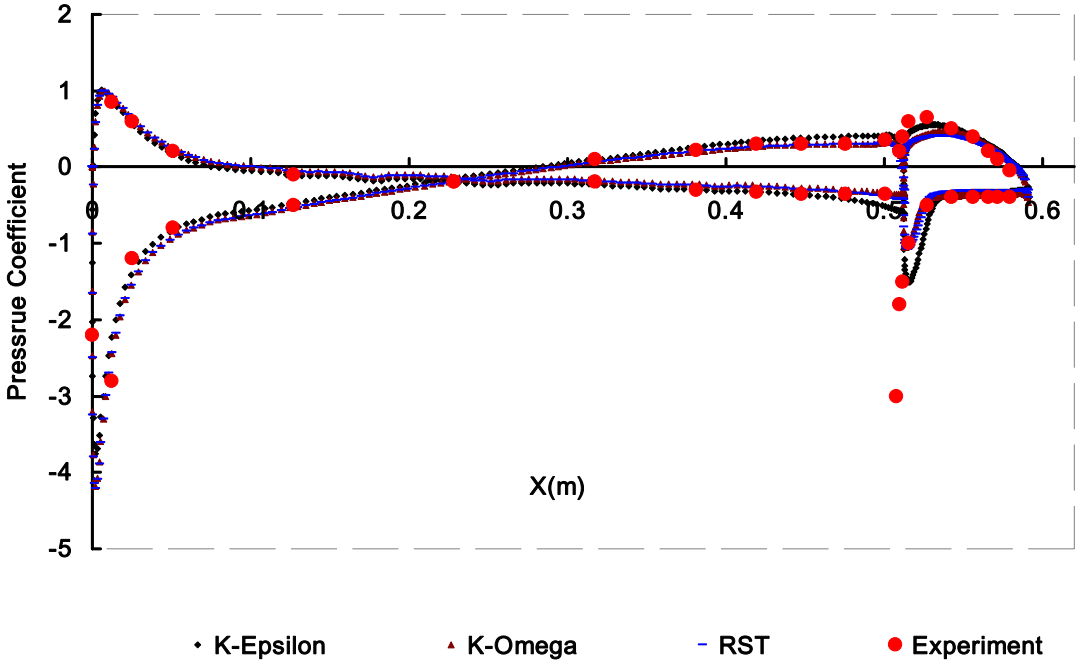

Fig. 13 Pressure coefficient C_p at -12.13^o attack angle with 40^o flap deflection

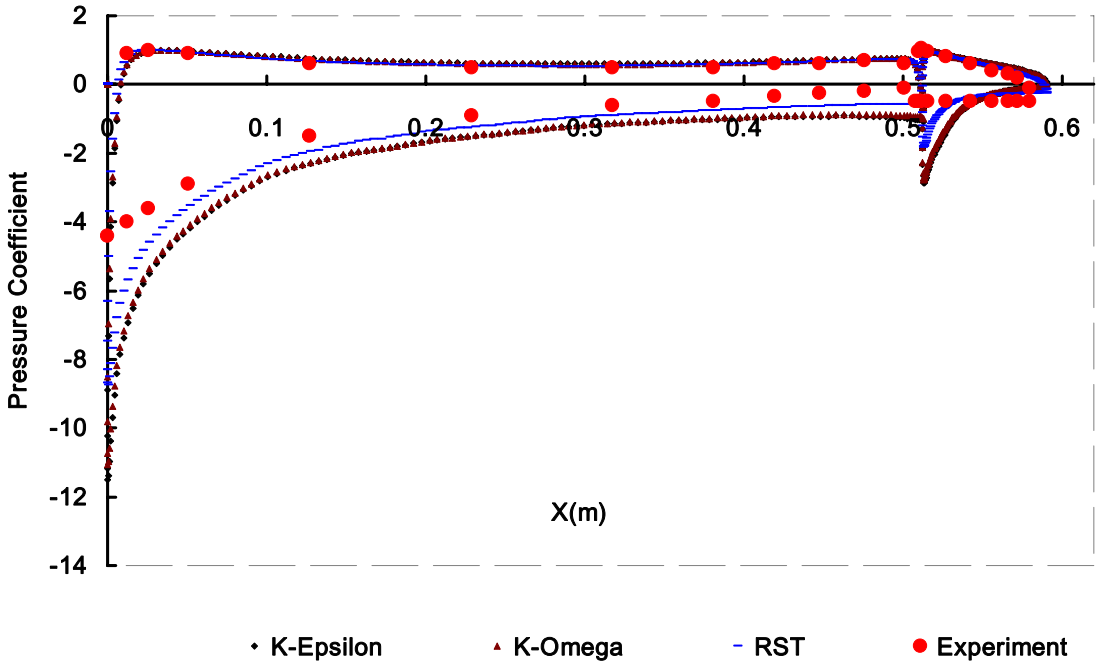

Fig. 14 Pressure coefficient C_p at 9.59^o attack angle with 40^o flap deflection

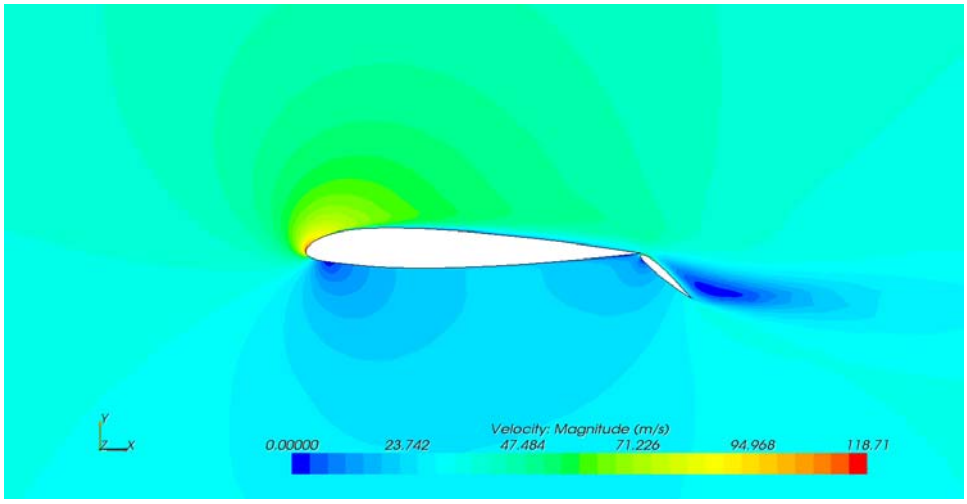

Fig. 15 Velocity magnitude contour at 9.59^o attack angle with 40^o flap deflection.

Conclusions

This paper has simulated flow over a NACA23012 airfoil with an external NACA23012 airfoil. The simulation was conducted in STAR-CCM+ with three turbulent models, which are *K*-ε, *K*-ω, and RST models. The simulation results are compared with wind tunnel data. Good agreements with the experimental data were found in low angle attacks for all the three turbulence models. Discrepancies increase when flow separates from the flap. In general RST gave the best results, but *K*-ω model also gave good results at a much lower computational cost.

Acknowledgement
This project is supported by the CT Space Grant Consortium.

Reference

1. Acosta, W.A. and Matty, J.J., "The NPARC Alliance: A Science and Technology/Test and Evaluation Partnership Example", NASA/TM-2000-210064, ARL-TR-2112, May 2000.
2. Bousman, W., "Airfoil Design and Rotorcraft Performance," Proceedings of the 58th Annual Forum of the American Helicopter Society, Montreal, Canada, June 11-13, 2002.
3. Smith, M.J., Wong, T.-C., Potsdam, M., Baeder, J., and Phansee, S., "Evaluation of CFD to Determine Two-Dimensional Airfoil Characteristics for Rotorcraft Applications," *AHS Journal*, January, 2006.
4. Johnson, F., Tinoco, E., and Yu, J., "Thirty Years of Development and Application of CFD at Boeing Commercial Airplanes", 16th AIAA Computational Fluid Dynamics Conference, June 23-26, Orlando, Florida, 2003.
5. Tangler, J.L., "The Nebulous Art of Using Wind-Tunnel Airfoil Data for Predicting Rotor Performance", Wind Energy, 5, 2002.
6. Iaccarino, Gianluca, "Predictions of a Turbulent Separated Flow Using Commercial CFD Codes", Journal of Fluids Engineering, Vol. 123, pp. 819-828, 2001.
7. Wenzinger, Carl J., "Pressure Distribution over an N.A.C.A. 23012 Airfoil with an N.A.C.A 23012 External-Airfoil Flap", Report No. 614, Langley Memorial Aeronautical Laboratory, National Advisory Committee for Aeronautics, Langley Field, VA, July 29, 1937.
8. Lift & Drag vs. Normal & Axial Force ,

http://www.aerospaceweb.org/question/aerodynamics/q0194.shtml

9. STAR CCM+ 3.04 User Manual, Cd-adapco.
10. Parezanovic, V., Rasuo, B., Adzic, M., "Design of Airfoils for Wind Turbine Blades", French-Serbian European Summer University : Renewable Energy Sources And Environment-Multidisciplinary Aspect, October 17-24, 2006, Vrnjačka Banja , Serbia.